

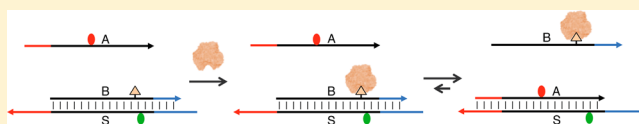
# A DNA-Mediated Homogeneous Binding Assay for Proteins and Small Molecules

Zhao Zhang,<sup>†</sup> Christian Hejesen, Michael B. Kjelstrup, Victoria Birkedal, and Kurt V. Gothelf\*

Center for DNA Nanotechnology (CDNA) at the Interdisciplinary Nanoscience Center (iNANO), Aarhus University, DK-8000 Aarhus C, Denmark

**S** Supporting Information

**ABSTRACT:** Optical detection of molecular targets typically requires immobilization, separation, or chemical or enzymatic processing. An important exception is aptamers that allow optical detection in solution based on conformational changes. This method, however, requires the laborious selection of aptamers with high target specificity and affinity, and the ability to undergo the required conformational changes. Here we report on an alternative generic scheme for detecting small molecules and proteins in solution based on a shift in the equilibrium of DNA-based strand displacement competition reaction. The shift occurs upon binding of a protein, for example, an antibody to its target. We demonstrate nanomolar detection of small molecules such as biotin, digoxigenin, vitamin D, and folate, in buffer and in plasma. The method is flexible, and we also show nanomolar detection of the respective antibodies or protein targets of these molecules. The detection scheme provides a generic alternative to aptamers for detection of analytes.



## INTRODUCTION

Detection of analytes in binding assays such as enzyme-linked immunosorbent assay (ELISA) relies on immobilization of the binding moiety, e.g., an antibody at a surface.<sup>1</sup> Homogeneous binding assays on the other hand can be performed in a single tube containing the specimen and all reagents, obviating any immobilization, separation, or washing steps, thus minimizing the chances of contamination.<sup>2</sup> Most of these assays are either based on aptamers,<sup>3,4</sup> or are limited to DNA-binding proteins.<sup>5,6</sup> Other assays such as quenchbodies,<sup>7,8</sup> binding-induced annealing<sup>9–13</sup> or proximity ligation,<sup>14–16</sup> often involve the events of multivalent binding or the procedure of DNA–protein conjugation. The method of fluorescence polarization is less general since it requires a fluorescent ligand.<sup>17</sup>

Here we report on a method for detection of small molecule or protein targets in homogeneous solution, which is based on the binding of a protein to a small molecule ligand conjugated to one of the strands in a DNA duplex. We have found that upon binding of streptavidin (STV) the melting temperature ( $T_m$ ) of the duplex decreases. As shown in Figure 1, the melting temperature of a duplex containing biotin attached to one of the bases (ds-1b) decreases around 10 °C after binding STV, which is even more than what is caused by a mismatch (Supporting Information Figure S1). Moreover, the  $T_m$  will decrease further when STV binds to two biotins on one strand, in which case part of the strand might tend to wrap around the protein via bivalent binding (Figure 1 and Figure S1).

Recently, Zhang et al. reported on a method to optimize the specificity in nucleic acid hybridization and to detect mismatches.<sup>18</sup> In this method, two DNA strands compete about the hybridization to a third strand which has toeholds<sup>19</sup> at each terminus unique for each of the competing strand. The introduction of a mismatch in one of the competing strands in

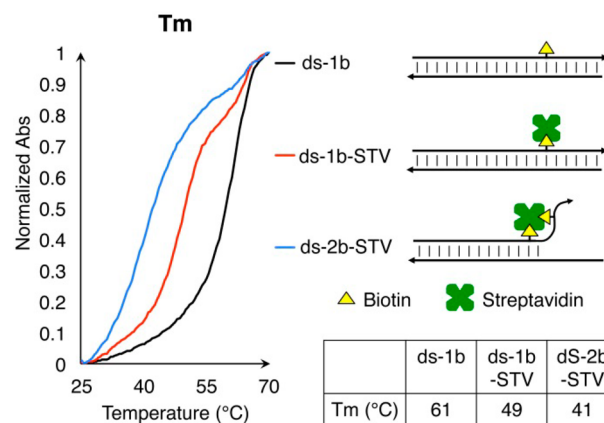


**Figure 1.**  $T_m$  change induced by ligand–protein binding on DNA duplex. (Left) Melting curves of a 18 bp DNA duplex with one biotin (black), one biotin and one streptavidin (STV) (red), or two biotins and one STV (blue). (Upper right) Illustration of each configuration. (Lower right)  $T_m$  derived from the curves.

the toehold exchange reaction results in a significant change of the equilibrium compared to the fully matched case.<sup>20</sup>

By implementing the ligand–protein induced changes of  $T_m$  in toehold exchange probes, we developed the strand displacement competition (SDC) assay for detection of proteins shown in Figure 2. Without target protein, the three strands, A, B modified with a ligand, and S, will reach a dynamic equilibrium which mainly depends on the  $T_m$  difference between AS and BS<sup>18</sup> (see Supporting Information Figure S2). If a protein target (T) binds to the small molecule conjugated

Received: June 2, 2014

Published: July 22, 2014

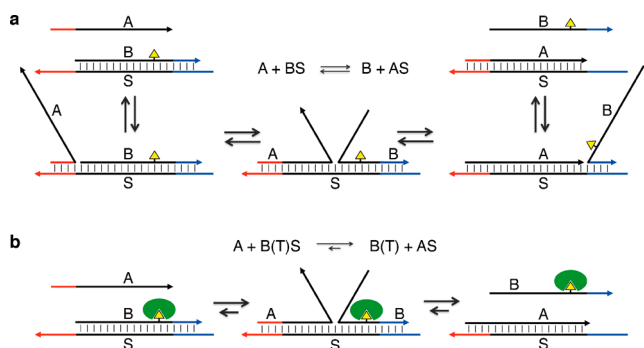


**Figure 2.** Detection of biomolecules based on the strand displacement competition assay. (a) Schematic illustration of the strand displacement competition reaction. Both strand A and strand B are complementary to a part of strand S, and they are mixed in a 1:1:1 ratio. In a typical pathway, A (or B) will displace B (or A) from S, through the process of toehold binding, branch migration, and toehold dissociation. This reaction keeps proceeding at both directions; thus, a dynamic equilibrium is reached after certain amount of time. (b) In the presence of target protein (T), which can bind to the ligand modified on strand B to form B(T), the final equilibrium will be shifted toward AS since the  $T_m$  of B(T)S is lower after binding.

to the B strand, the equilibrium shifts due to decrease of the  $T_m$  of B(T)S, thus more AS will be formed. The population change can be detected by PAGE or by an optical signal such as Förster resonance energy transfer (FRET) if dyes are conjugated to the DNA strands. This binding-induced blocking mechanism also relates to Plaxco et al.'s electrochemical sensor,<sup>21</sup> however, in that assay immobilization is a requirement.

## EXPERIMENTAL SECTION

**Materials.** All the modified and unmodified oligonucleotides except two were purchased from DNA Technology A/S (Denmark) or Sigma-Aldrich (St. Louis, MO). HPLC purification was performed by the supplier directly after synthesis. The DNA strand with a shorter linker for the amino modifier (B4a2-2) was synthesized in-house on a Mermade-12 DNA synthesizer (BioAutomation, TA), using the 5-aminoallyl-dU phosphoramidite (Berry & Associates, Dexter, MI) according to instructions. The DNA strand with a 2'-amino modification was bought from IBA (Germany) and purified by HPLC. The concentration of each oligonucleotide was measured by Nanodrop 1000 spectrophotometer (Thermo Fisher Scientific, Cambridge, MA).

Alexa Fluor Succinimidyl Esters (647, 555 and 488) were purchased from Invitrogen (Carlsbad, CA). Polyclonal anti-digoxigenin from sheep was purchased from Roche Applied Science (Germany). Adenosine 5'-triphosphate (ATP) was purchased from New England Biolabs (Ipswich, MA). Monoclonal anti-folic acid antibody from mouse was purchased from Acris Antibodies (Germany). Folic Acid-N3 was purchased from Baseclick (Germany). All the other reagents were purchased from Sigma-Aldrich.

**UV Absorbance Melting Studies.** Absorbance vs melting temperature curves were recorded at 260 nm on a Varian Cary 100 spectrophotometer (Palo Alto, CA), in thermal mode. All melting curves were recorded in 1× TAE buffer (40 mM Tris, 1 mM EDTA, pH 8) containing 12.5 mM  $MgCl_2$ , at a standard concentration of 1  $\mu M$ . A ramp rate of 0.5 °C/min was used and the block underwent two repeated thermal cycles from 25 to 70 °C then back to 25 °C. Data of the second cycle from 25 to 70 °C was collected and analyzed by using derivative calculations. All melting temperatures were recorded in duplicate and they varied by less than 1 °C in all cases.

**Construction of the SDC Assay for Protein Detection.** 0.5 mL BILATEC tubes (Sigma-Aldrich) were used for all the reactions. A typical SDC assay was prepared by simply mixing DNA strand A, B

and S or their equivalents in equal stoichiometric ratio (70  $\mu L$ , 20 nM), in 1× TAE/ $Mg^{2+}$  buffer pH 8. The target protein or control (usually water) was also added at the same time. Then the whole mixture was incubated at room temperature (RT) overnight in the dark. Since this method is based on thermodynamics instead of kinetics, the order of addition of different components is irrelevant to the final readout.

**Construction of the SDC Assay for Small Molecule Detection.** As illustrated in Supporting Information Figure S12, two strategies can be adopted for this purpose. In the inhibition strategy, the specimen with or without analyte molecules was premixed with the corresponding protein first. After incubation at room temperature (RT) for 3 h, the mixture was added into the standard SDC assay and incubated at RT overnight in the dark. In the replacement strategy, the protein and assay are mixed first and left at RT overnight. The specimen is then added and the mixture incubated at RT for another 5 h.

**FRET Experiments.** Fluorescence measurements were performed using a scanning spectrofluorometer (Fluoro-Max-3, HORIBA Jobin Yvon Inc.). The assay-specimen mixture was pipetted into a quartz cuvette (65  $\mu L$ ), which was washed by 1× TAE/ $Mg^{2+}$  three times between different samples. All spectral measurements were recorded with 0.5 s integration time and 1 nm wavelength interval, at 25 °C.

For the FRET pair of Alexa555 and Alexa647 as in most assays, excitation was performed at 550 nm for Alexa555. Relative FRET efficiencies were calculated as  $E_r = I_{DA}/(I_{DA} + I_{DD})$ , where  $I_{DA}$  is the acceptor peak fluorescence intensity at 667 nm and  $I_{DD}$  is the donor peak fluorescence intensity at 567 nm.

For the three-dye system, excitation was performed at 450 nm for Alexa488, 550 nm for Alexa555, and 600 nm for Alexa647. Relative FRET efficiency of the pair of Alexa488 and Alexa555 was calculated as  $E_r = I_{D1A1}/(I_{D1A1} + I_{D1D1})$ , where  $I_{D1A1}$  is the acceptor peak fluorescence intensity at 567 nm and  $I_{D1D1}$  is the donor peak fluorescence intensity at 519 nm. Relative FRET efficiency of the pair of Alexa555 and Alexa647 was calculated as  $E_r = I_{A2A2}/I_{D2A2}$ , where  $I_{A2A2}$  is the acceptor peak fluorescence intensity at 667 nm when Alexa555 is excited, and  $I_{D2A2}$  is the acceptor peak fluorescence intensity at 667 nm when Alexa647 is excited.

For the real-time FRET measurement, the pair of Alexa488 and Alexa555 was used. Fluorescence was recorded at 519 nm (Alexa488) and 567 nm (Alexa555) with an excitation at 450 nm, at a time interval of 60 s. Relative FRET efficiencies were calculated as  $E_r = I_{DA}/(I_{DA} + I_{DD})$ , where  $I_{DA}$  is the acceptor peak fluorescence intensity at 567 nm and  $I_{DD}$  is the donor peak fluorescence intensity at 519 nm.

**Nondenaturing Polyacrylamide Gel Electrophoresis (PAGE).** Mixtures of sample (0.16 pmol for each strand) and 6× nondenaturing loading buffer (0.25% bromophenol blue +30% glycerol) were loaded on native PAGE gel (acrylamide/bisacrylamide; 19:1, 6%), which was run in a fridge using a PowerPac 1000 power supply (Bio-Rad) (70 V, 1.5 h). TBE/ $Mg^{2+}$  (1×; 12.5 mM) was used for both gel and running buffer.

**Typhoon Scanning.** After electrophoresis, the gel was scanned by Typhoon scanner (Amersham Biosciences) without staining. Red laser (633 nm) for excitation and 670 nm band-pass filter for emission were chosen. The scanned gels were analyzed by ImageQuant TL 7.0 (GE Healthcare). Lane creation and band detection were done manually. Since Alexa647 was mostly modified on strand A, the intensity of the bands only represent the amount of A. Normally there are two detectable bands: the upper band is A in the form of AS duplex, while the lower band is single-stranded A (ssA). We use the value of  $ssA/(ssA + AS)$  as a robust indicator for evaluation of the population change in solution.

## RESULTS

**Detection of Proteins: Streptavidin.** We first tested this strategy for detection using the strong biotin-STV interaction as a model. As shown in Figure 3a, strands A, B, and S were mixed in equal stoichiometry, among which, A and S each are labeled

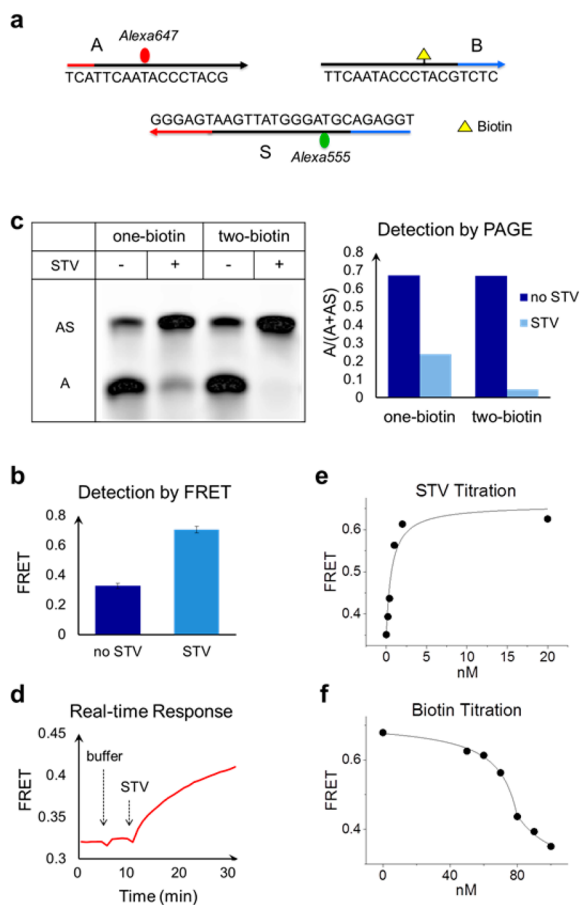


**Figure 3.** Detection of streptavidin (STV) and biotin as a model system. (a) Schematic illustration of the SDC assay based on biotin-STV interaction. (b) FRET results of STV detection. In the presence of excessive STV, FRET signal increased more than 1-fold, indicating more AS are formed. (c) Gel scanned on a Typhoon scanner. Left two lanes are the system shown in (a), while right two lanes are a two-biotin system shown in Supporting Information Figure S5. The band intensity reflects the amount of A, since only the dye of Alexa647 on A is excited and emitted. Upper and lower band represent AS and ssA, respectively. The effect of STV was evaluated and compared using the percentage of ssA in total A. (d) Time-dependent FRET for STV detection. (e) Titration curve of STV detection ( $[A] = [B] = [S] = 7$  nM). All the data are fit by a hyperbolic function. The same below. (f) Titration curve of biotin detection by the inhibition method ( $[A] = [B] = [S] = 14$  nM,  $[STV] = 20$  nM).

with fluorophores forming a FRET pair, while B is conjugated to biotin which serves as the binding moiety for STV detection.

All the modifications are located on the branch migration region. A and B endow 3 nt and 4 nt toeholds, respectively; therefore, without STV, BS has slightly lower standard free energy than AS. Upon binding of STV, the melting temperature of the BS duplex decreases, resulting in a shift of the equilibrium toward the AS duplex. This event can be observed by both FRET (Figure 3b) and PAGE (Figure 3c). Here the FRET signal is linked to the population of AS, while the gel shows the ratio of A in single-stranded (ss) and double-stranded (ds) form in the solution. It is observed that STV causes the emergence of more AS and less ssA, which is consistent with the scheme. The amount of BS is confirmed to decrease in a three-dye system where strand B also has a fluorophore (Supporting Information Figure S3).

The position of the ligand on B is important for the effect of target binding and it was observed that the optimal position is in the branch migration region (Supporting Information Figure S4). By making use of the tetravalency of STV, we also conjugated two biotins on one strand (Supporting Information Figure S5), which results in even lower  $T_m$  of BS after bivalent binding to STV (Figure 1). Both FRET and gel results showed that in this two-biotin system, a higher amount of AS was formed than in the one-biotin system in the presence of STV, and only negligible single-stranded A was left (Figure 3c and Supporting Information Figure S4).

The effect of target binding depends on the stoichiometry of A, B and S. However, we found that other ratios than 1:1:1 can also ensure significant effect of STV, although the absolute FRET value is different (Supporting Information Figure S6). Furthermore, it is worth noting that after normalization with reference samples containing only AS or BS, the FRET signal change became even more significant (Supporting Information Figure S7).

The sensor specificity was tested by adding a variety of other proteins, which should not interact with biotin to the biotin assay, and none of them displayed any significant effect on the equilibrium (Supporting Information Figure S8). When adding various proteins into a control system without ligand on the DNA strands, no FRET signal change was observed, validating the robustness of the system (Supporting Information Figure S9).

To make sure the SDC reaction reaches equilibrium, unless otherwise specified, all the reactions in this study were left to proceed at RT overnight, although the time-dependent FRET measurement revealed that the FRET signal has already halfway changed in the first half an hour (Figure 3d). Elongating the toehold length on both A and B is expected to increase the rate of the equilibrium,<sup>22</sup> but our study also revealed that longer toeholds lead to decreased FRET signal (Supporting Information Figure S10).

The FRET signals of a 7 nM assay in response to STV of increasing concentrations within the range of 0 to 2 nM are shown in Figure 3e. The detection limit of this assay relies on the sensitivity of the fluorometer, as well as the rate constant which is dependent on concentration.<sup>22</sup> We have demonstrated that by PAGE it was possible to detect as low as 125 pM streptavidin (Supporting Information Figure S11).

**Small Molecule Detection: Biotin.** The SDC assay can be extended to detection of small molecules similar to the ligand conjugated to the B strand, using an inhibition or a replacement method (Supporting Information Figure S12). In the former detection mode, a known concentration of the protein is incubated with a sample containing an unknown concentration of the ligand and this mixture is applied to the SDC assay. This method was applied to the STV-biotin assay for the detection of biotin. In the absence of biotin as target molecule, STV will exert the same effect on the equilibrium as before. If the sample contained biotin, it will block the corresponding binding-sites on STV, thereby decreasing the number of sites that can bind to the biotin-DNA conjugate (strand B) in the assay (Supporting Information Figure S13). Figure 3f shows the measured FRET efficiency using 14 nM of DNA, 20 nM of STV, and a series of concentrations of biotin. The curve reflects the tetravalency of streptavidin as the dynamic range is in the interval of 60–80 nM biotin, where the last binding site of STV is occupied. In the alternative *Replacement method* (Supporting Information Figure S12), the sample containing the small

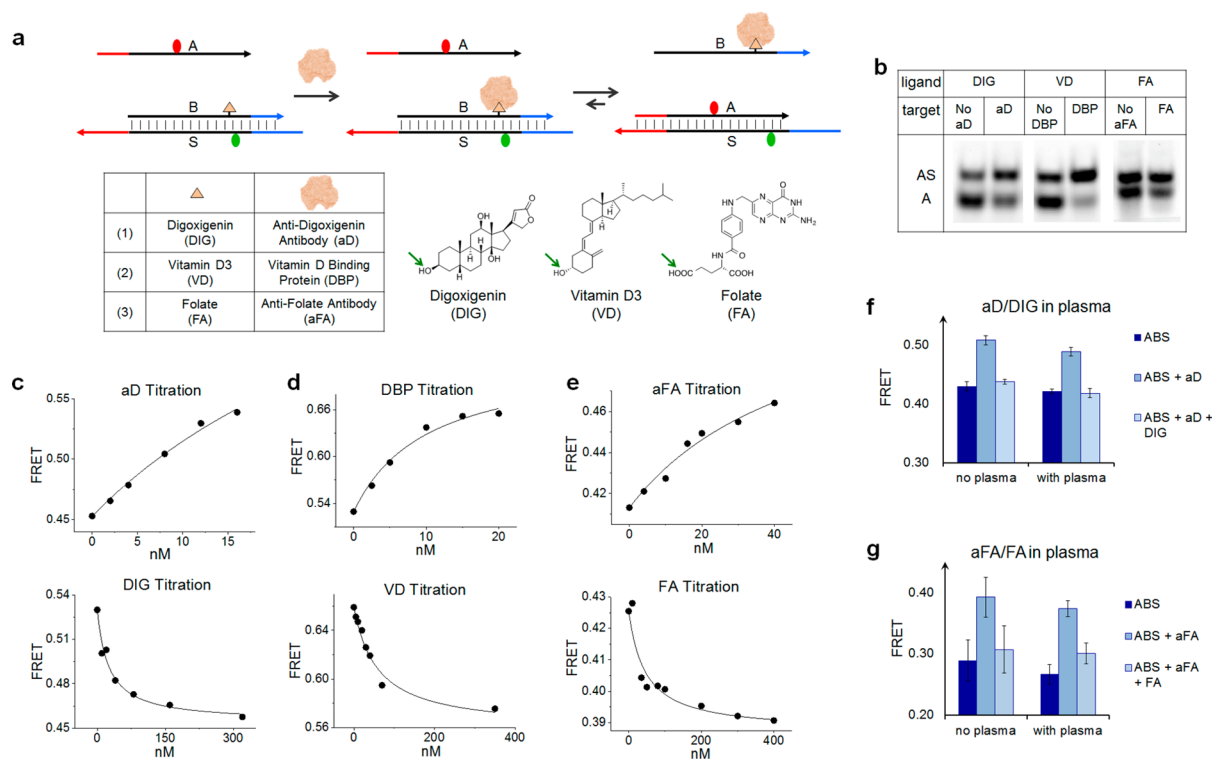


**Figure 4.** Detection of digoxigenin, vitamin D, folate and their respective protein/antibody binders. (a) Schematic illustration of the SDC assay. The functional group that is used for conjugation to DNA is indicated with a green arrow. (b) Gel characterization of the effect of aD, DBP and aFA. The intensity of bands represents the amount of strand A. More AS duplex and less ssA emerged after protein binding. (c–e) FRET results for titration of aD and DIG, VD and DBP, and aFA and FA. Small molecules were detected using the inhibition method. (f and g) Bar plots comparing the detection of aD and DIG, and aFA and FA in buffered samples and samples containing 14% human plasma.

molecule can be added directly to the SDC assay containing the protein to replace the small molecules conjugated to DNA bound to the protein with the small molecule target in solution. The replacement method requires a reversible exchange of ligands bound to the protein and cannot be applied to the biotin-STV assay since the off rate is too low. Therefore, only the inhibition method was tested for detection and quantification of biotin.

**Detection of 3 Other Proteins/Antibodies and Their Small Molecule Targets.** After having obtained proof of concept for the SDC assay for detection of the very strong biotin-STV interaction, we have extended it to detect other small molecule-protein interactions. Three pairs of interactions were examined: digoxigenin (DIG)/antidigoxigenin (aD), vitamin D<sub>3</sub> (VD)/vitamin D binding protein (DBP), and folate (FA)/antifolate (aFA) (Figure 4). The former pair was chosen as model for antigen-antibody binding, while both vitamin D and folate (Vitamin B<sub>9</sub>) levels in the body are crucial to human health and corresponding deficiency can cause serious diseases.<sup>23–25</sup>

The three molecules DIG, VD and FA were conjugated to amino-modified strand B (Figure 4a). However, when using the standard C6 linker between the modified DNA base and the small molecules that was used for biotin no changes in equilibria were detected when the corresponding binding proteins were added (Supporting Information Figure S14). To increase the impact of the interaction on the DNA strand, a dT amino modifier with a shorter C3 linker was employed for this purpose,<sup>26</sup> and the protein binding events were confirmed by PAGE (Supporting Information Figure S15). The feasibility of another linker where the amine group is directly modified on

the C2' of the deoxyribose was also confirmed (Supporting Information Figure S16).

The changes in equilibrium caused by the addition of the corresponding proteins/antibodies were analyzed by PAGE as shown (Figure 4b). The changes in equilibrium are less pronounced than the biotin streptavidin interaction, however still significant, in particular for the binding of DBP to VD. We believe the smaller change in FRET is caused by a smaller change in T<sub>m</sub> upon protein binding. It was not possible to obtain T<sub>m</sub> curves for DIG and DBP due to denaturation of the proteins; however, for the aFA/FA couple, we observed a change in T<sub>m</sub> of 3 °C in the presence of excess of the protein. This corresponds well with the smaller change in FRET for the aFA/FA couple. The FRET response to titration of increasing concentrations of aD, DBP and aFA are shown in Figure 4c–e. For these assays the concentration of the ABS strands were 20 nM and it was observed that all three titration curves have the dynamic ranges from approximately 1 to 20 nM. The specificity of each assay was confirmed by the absence of equilibrium shifts upon adding other proteins to the assays (Supporting Information Figure S17). With the inhibition method, the small molecules DIG, VD and FA can also be detected by premixing the small molecules and the corresponding protein followed by addition to the SDC assay (Figure 4c–e). As it appears from the titration curves, the small molecules can be detected by FRET, and the assays have dynamic ranges of approximately 10–100 nM using the current setup. The replacement method by which the specimen is added directly into the assay mixture including proteins can also be adopted for detection of the small molecules (Supporting Information Figure S18). The free

ligands will compete with the ligands on strand B to bind with proteins, thus have the opposite effect on the equilibrium.

**Human Plasma and Saliva.** Finally, the SDC assay was tested for detection of the 6 analytes in 14% human plasma. First it was attempted to examine the VD/DBP assay. However, since the albumins in plasma bind to Vitamin D the equilibrium shifted significantly in plasma and as a result neither VD nor DBP could be detected. On the other hand, the detection of aD and DIG and aFA and FA was feasible in plasma. For these experiments, 14% plasma spiked with the target compounds was used. Due to the numerous different constituents of human plasma, PAGE was not suitable for monitoring the equilibrium in plasma. The equilibrium changes were, however, clearly detectable by FRET. As shown in Figure 4f,g, the addition of plasma to the ABS system has only minor impact on the equilibrium. The shift in FRET observed after addition of 2 equiv of aD is almost similar for the systems in plasma and in buffer. For the detection of digoxigenin, addition of 10 equiv of DIG to the ABS system and subsequent addition of aD shows almost similar results in buffer and in plasma. Detection of aD and DIG was also demonstrated in 84% plasma and in 14% saliva (Supporting Information Figure S19).

## DISCUSSION

The method appears to be general for detecting biomolecular interactions involving small molecules and proteins as shown for the couples of biotin/STV, DIG/aD, VD/DBP and FA/aFA. However, the optimal length of the tether between the DNA B sequence and the small molecule target seems to be crucial and differs from protein to protein. This is probably caused by different local configurations of the ligand–protein interactions. We believe that the decrease of the  $T_m$  of the binding duplex is mainly caused by steric repulsion between the protein and the binding site in the major groove of the DNA helix. Meanwhile, electrostatic interactions may also be important for the interaction. In both cases, the more proximal the protein is to the DNA components upon binding to the ligand, the larger effect it will potentially have on the equilibrium. The biotin-binding pocket in streptavidin is buried relatively deep inside the protein,<sup>27</sup> and therefore, the effect is obtained with the relatively long C6 linker between the DNA base and biotin. For the antibody/small molecule interactions, the binding site is generally located at the surface of the antibody,<sup>28</sup> and thus, a shorter linker between the DNA B strand is required to obtain a sufficient repulsion to shift the equilibrium in the SDC assay. We believe this is also the case for the VD/DBP couple.<sup>29</sup>

The position of the small molecule ligand in the DNA B sequence also appeared to be crucial for the equilibrium shift induced upon binding of the protein as shown in Supporting Information Figure S4. A ligand placed in the branch migration region will shift the sensor equilibrium more significantly than when positioned in the toehold region, while a ligand placed at the terminal of the strand has almost no effect. This is in accordance with the relation reported for the position of single point mismatches in short DNA duplexes and their  $T_m$ .<sup>30</sup> The maximum decrease of  $T_m$  was observed when the mismatch was at the center of the sequence.

The SDC method allows detection of small molecule–protein interaction in homogeneous solution without the need of immobilization or separation procedures and in that regard the method compares to aptamers. The major advantage of the SDC method is that no selection is required since existing

binding interactions between proteins (antibody) and small molecule can be applied, although it does require that the small molecule can be linked to the oligonucleotide without significantly decreasing the binding affinity to the protein. In most cases, the conformational change of aptamers required for providing an optical readout from a homogeneous solution is another challenge and often requires substantial structural analysis and structural engineering of selected aptamers. The SDC system is, on the other hand, predesigned to make the shift of equilibrium upon binding of the protein to the small molecule ligand and the FRET couple is thereby completely separated. Furthermore, the same sequences can be used for all targets in the SDC assay. Adjustment of the initial equilibrium can easily be achieved by adding or deleting bases in the toehold region of sequence A or B.

The sensitivity of the SDC method is dependent on (i) the affinity of the protein to the small molecule–DNA conjugate, (ii) the concentration of the DNA sequences in the assay, (iii) the emission from the FRET couple at the given concentration, and (iv) the equilibrium shift. At the current state of development of the assay, the main limiting factor is detection of the emission from the FRET couple at low concentration of the DNA assay. In the data presented here, the detection limit for proteins/antibodies is in the low nanomolar range by FRET and down to 125 pM by PAGE. In several cases, DNA and RNA aptamers that bind to proteins with affinities in the picomolar range have been selected.<sup>31</sup> The SDC may, however, have potential to reach similar low affinities for protein binding by optimizing the FRET dyes. For small molecule, aptamers with nanomolar sensitivity have been selected, however, in most cases the affinities are micromolar.<sup>32</sup> The examples shown here by the SDC method demonstrate sensitivity in the nanomolar regime in all cases, and as for the protein detection, we also believe that the sensitivity of small molecule binding can be further optimized.

## CONCLUSION

We introduced a method to detect small molecule analytes and proteins, e.g., antibodies in homogeneous solutions with high specificity. By the direct binding of a protein target to a small molecule in the SDC assay, quantitative detection of nM concentrations of proteins can be obtained by fluorescence or PAGE. Small molecules can also be detected by incubation with a known concentration of the respective protein, thus outcompeting the binding to the identical DNA linked small molecule. The competitive nature of the assay makes the equilibrium highly invariable to changes in the environment such as concentration, salts, temperature, etc.<sup>18</sup> As an example, we showed that the SDC assay could be applied for detection of antibody and its small molecule hapten in plasma or saliva. In perspective, we believe that the method can be extended to other small molecules and protein couples and the detection scheme has potential for application in clinics for quantification of disease biomarkers, in human plasma.

## ASSOCIATED CONTENT

### Supporting Information

DNA sequences, supplementary schemes (S1–S3) and additional results (Figures S1–S19). This material is available free of charge via the Internet at <http://pubs.acs.org>.

## AUTHOR INFORMATION

### Corresponding Author

kvg@chem.au.dk

### Present Address

<sup>†</sup>Nanobiology Institute, Yale University, West Haven, CT 06516, USA.

### Notes

The authors declare the following competing financial interest(s): The authors of the manuscript have filed a patent application covering the main concepts of the work presented here. The PCT application WO2014041024 was published on May 20, 2014 under the title: Detection of non-nucleic acid analytes using strand displacement exchange reactions.

## ACKNOWLEDGMENTS

This research was supported by grants from the Danish National Research Foundation to Center for DNA Nanotechnology (DNRF81) and the Danish Council for Independent Research for a Sapere Aude Grant (V.B.) and an Eliteforsk Award (K.V.G.).

## REFERENCES

- (1) Lequin, R. M. *Clin Chem.* **2005**, *51*, 2415.
- (2) Zhang, H.; Li, F.; Dever, B.; Li, X. F.; Le, X. C. *Chem. Rev.* **2013**, *113*, 2812.
- (3) Nutiu, R.; Li, Y. *J. Am. Chem. Soc.* **2003**, *125*, 4771.
- (4) Sassolas, A.; Blum, L. J.; Leca-Bouvier, B. D. *Analyst* **2011**, *136*, 257.
- (5) Wang, J.; Li, T.; Guo, X.; Lu, Z. *Nucleic Acids Res.* **2005**, *33*, e23.
- (6) Leung, C. H.; Chan, D. S.; He, H. Z.; Cheng, Z.; Yang, H.; Ma, D. L. *Nucleic Acids Res.* **2012**, *40*, 941.
- (7) Abe, R.; Ohashi, H.; Iijima, I.; Ihara, M.; Takagi, H.; Hohsaka, T.; Ueda, H. *J. Am. Chem. Soc.* **2011**, *133*, 17386.
- (8) Abe, R.; Jeong, H. J.; Arakawa, D.; Dong, J.; Ohashi, H.; Kaigome, R.; Saiki, F.; Yamane, K.; Takagi, H.; Ueda, H. *Sci. Rep.* **2014**, *4*, 4640.
- (9) Heyduk, E.; Dummit, B.; Chang, Y. H.; Heyduk, T. *Anal. Chem.* **2008**, *80*, 5152.
- (10) Lundberg, M.; Eriksson, A.; Tran, B.; Assarsson, E.; Fredriksson, S. *Nucleic Acids Res.* **2011**, *39*, e102.
- (11) Li, F.; Zhang, H.; Wang, Z.; Li, X.; Li, X. F.; Le, X. C. *J. Am. Chem. Soc.* **2013**, *135*, 2443.
- (12) Li, F.; Zhang, H.; Lai, C.; Li, X. F.; Le, X. C. *Angew. Chem., Int. Ed.* **2012**, *51*, 9317.
- (13) Zhang, H.; Li, F.; Dever, B.; Wang, C.; Li, X. F.; Le, X. C. *Angew. Chem., Int. Ed. Engl.* **2013**, *52*, 10698.
- (14) Fredriksson, S.; Gullberg, M.; Jarvius, J.; Olsson, C.; Pietras, K.; Gustafsdottir, S. M.; Ostman, A.; Landegren, U. *Nat. Biotechnol.* **2002**, *20*, 473.
- (15) Fredriksson, S.; Dixon, W.; Ji, H.; Koong, A. C.; Mindrinos, M.; Davis, R. W. *Nat. Methods* **2007**, *4*, 327.
- (16) Gustafsdottir, S. M.; Schlingemann, J.; Rada-Iglesias, A.; Schallmeiner, E.; Kamali-Moghaddam, M.; Wadelius, C.; Landegren, U. *Proc. Natl. Acad. Sci. U.S.A.* **2007**, *104*, 3067.
- (17) Rossi, A. M.; Taylor, C. W. *Nat. Protoc.* **2011**, *6*, 365.
- (18) Zhang, D. Y.; Chen, S. X.; Yin, P. *Nat. Chem.* **2012**, *4*, 208.
- (19) Yurke, B.; Turberfield, A. J.; Mills, A. P., Jr.; Simmel, F. C.; Neumann, J. L. *Nature* **2000**, *406*, 605.
- (20) Werntges, H.; Steger, G.; Riesner, D.; Fritz, H. J. *Nucleic Acids Res.* **1986**, *14*, 3773.
- (21) Cash, K. J.; Ricci, F.; Plaxco, K. W. *J. Am. Chem. Soc.* **2009**, *131*, 6955.
- (22) Zhang, D. Y.; Winfree, E. *J. Am. Chem. Soc.* **2009**, *131*, 17303.
- (23) DeLuca, H. F. *Am. J. Clin. Nutr.* **2004**, *80*, 1689S.
- (24) Holick, M. F. *N. Engl. J. Med.* **2007**, *357*, 266.
- (25) Board, N. A. o. S. I. o. M. F. a. N. In *Dietary Reference Intakes for Thiamin, Riboflavin, Niacin, Vitamin B6, Folate, Vitamin B12,*

*Pantothenic Acid, Biotin, and Choline*; National Academy Press.: Washington, D.C., 1998; p 196.

(26) Lermer, L.; Roupioz, Y.; Ting, R.; Perrin, D. M. *J. Am. Chem. Soc.* **2002**, *124*, 9960.

(27) Hendrickson, W. A.; Pahler, A.; Smith, J. L.; Satow, Y.; Merritt, E. A.; Phizackerley, R. P. *Proc. Natl. Acad. Sci. U.S.A.* **1989**, *86*, 2190.

(28) Al-Lazikani, B.; Lesk, A. M.; Chothia, C. *J. Mol. Biol.* **1997**, *273*, 927.

(29) Verboven, C.; Rabijns, A.; De Maeyer, M.; Van Baelen, H.; Bouillon, R.; De Ranter, C. *Nat. Struct. Biol.* **2002**, *9*, 131.

(30) Guo, Z.; Liu, Q.; Smith, L. M. *Nat. Biotechnol.* **1997**, *15*, 331.

(31) Hermann, T.; Patel, D. J. *Science* **2000**, *287*, 820.

(32) McKeague, M.; Derosa, M. C. *J. Nucleic Acids* **2012**, *2012*, 748.